Exploration of HSPC aging mechanism based upon in vitro cell modeling and MDS clinical sampling

Haiyan Hu
Shanghai University of Traditional Chinese Medicine
Xiangrong Song
Sichuan University
Lin Zhao
Shanghai University of Traditional Chinese Medicine
Lanyue Hu
Fujian Institute of Hematology, Fujian Medical University Union Hospital
Chu Xu
Shanghai Jiaotong University School of Medicine
Yanjuan Lin
Fujian Institute of Hematology, Fujian Medical University Union Hospital
Manying Zhou
Shanghai University of Traditional Chinese Medicine
Xiaolan Lian (L072073@163.com)
Fujian Institute of Hematology, Fujian Medical University Union Hospital
Lina Zhang
Shanghai University of Traditional Chinese Medicine

Research Article

Keywords: Myelodysplastic Syndromes (MDS), Hematopoietic aging, mRNA splicing, Hematopoietic stem/progenitor cell(HSPC)

Posted Date: September 2nd, 2022

DOI: https://doi.org/10.21203/rs.3.rs-2007552/v1

Abstract

Background

The pathogenetic mechanisms of Myelodysplastic Syndromes (MDS) were undefined. Hematopoietic senescence was manifested by association with malignant myeloid blood diseases, aging and immune dysfunction. Hematopoietic stem/progenitor cell (HSPC) aging was the primary determinant of hematopoietic senescence.

Methods

In current study, we used an in vitro HSPC aging mouse model that readily enabled the gather of a large number of aging HSPCs. The followed studies covered mRNA splicing and epigenetics (H3K27me3) relevant to HSPC aging, with methods such as Cut-tag, SA-β-gal assay, CFU-mix assay, RNA-seq, and RNAi knock down (KD).

Results

The results showed that HSPC aging associated down-regulation of SR and hnRNPs family genes and mRNA splicing inhibitor (SSA) elicited HSPC aging-like phenotype. Cut-tag assay demonstrated that HSPCs aging was linked to global decline in H3K27me3 levels, which however, was systemically up-regulated in occupying the promoter of SR family and hnRNPs family genes. In addition, HSPCs aging exhibited alterations in the splicing patterns of TSS and SKIP.

Conclusions

Together, we proposed the linkages of HSPCs aging with epigenetic repression of SR and HnRNPs genes and inhibition of mRNA splicing pathway to alter TSS and SKIP-relevant alternative splicing. Our study provided insights to the etiopathology of MDS by exposing its connections to HSPC aging.

Introduction

Although blood is a definitive self-renewing tissue of the body, it did not escape the aging process[[1–4]. Hematopoietic aging is manifested in human populations in the form of myeloproliferative diseases, including leukemias, declining adaptive immunity, and greater propensity to anemia[1, 5]. So it was of clinical imminence to address the mechanisms of hematopoietic senescence for the purposes of prevention and treatment. It is well established that most mature blood cells were constantly generated and replaced from hematopoietic stem cells (HSCs) through a series of lineage-committed hematopoietic progenitor cells (HPCs)[6–8], so mammals maintained hematopoiesis through the activity of thousands of hematopoietic stem and progenitor cells (HSPCs)[9–10]. It is accumulatively documented that age-related alterations in the human blood system depended on HSPCs aging [6–7, 11].

In vitro HSPC aging model is an important platform to study HSC/HPC-relevant senescence and associated diseases. In our early work, we established an *in vitro* cell model that enables to readily obtain a large amount of senescent HSPCs (China Patent No. 201711157564.6). We might even say it is an *in vitro* HSPC aging accelerating model when compared with the *in vivo* counterpart[12]. Based on this model, our previous studies with ITRAQ proteomics and transcriptomics showed that mRNA splicing was one prominent differential pathway between young and aging HSPCs groups. Therefore, we hypothesize that mRNA splicing disorder underlies HSPC aging and our proposal is supported by increasing evidences. Indeed, dysregulation of mRNA splicing was linked to aging and aging-related degenerative diseases[13–14]. Consistently, genome-wide splicing profile is a better predictor of biological aging than the gene and transcript expression profiling[15]. Although the De Almeida group has initiated a study on aging, mRNA splicing, and epigenetics[16], the mechanistic linkage between mRNA splicing and HSPC aging is barely substantialized. Nevertheless, our Lab has reported that total H3K27me3 level was significantly decreased in this patent model, as compared with the young group control[12].

MDS was viewed as the most relevant blood disease of hematopoietic senescence and the process of hematopoietic aging would qualitatively mimic MDS [17, 30]. In any case, a causal link has not be affirmed between HSPC senescence and CDS pathogenesis, which features in heterogeneous myeloid disorders characterized by peripheral blood cytopenias and susceptibility to AML transformation[18]. The clinical manifestations of MDS varied significantly with poor overall prognosis, conferring both challenges and urgency to seek test models and key mechanisms to advance the basic and therapeutical researches. In our current report, we assessed the pathological mechanisms of MDS based on *in vitro* and *in vivo* HSPC aging models.

Materials And Methods

Animals

Equal numbers of male and female C57BL/6J SPF mice were obtained from Shanghai Sippr-BK Experimental Animal Center [Certificate No. SCXK (Shanghai) 2013-0016]. The mice were 4 weeks in age and 16–18 g in weight. All animal experiments were performed in compliance with guidelines of the Animal Care and Use Committee of SHUTCM.

Materials

Red blood cell lysis buffer and SA-β-Gal staining kit were from Beyotime Biotechnology Co.. Lineage Cell Depletion kit and Anti-c-kit(CD117) MicroBead kit were from Miltenyi Biotec Co..RNA Extraction and Purification kit, Reverse Transcription and Fluorescence Quantitative PCR kit were from Takara Co.. Stemspan Stem Cell Media and Mouse Colony-Forming Unit (CFU) Assays MethoCult™ were from Stem cell Co..mouse SCF, IL-3 and IL-6 were from Novus Biologicals Co.. antibodies for PTB, HnRNPa0, HnRNP a2/b1, Rbmxl1, Pabpc1, Srsf1, Srsf3, Srsf5, and Srsf7 were from Thermo Fisher Scientific Co.. antibodies

for Srsf2, Srsf4, Srsf6, Srsf9 and Srsf11 were from Abcam Co.. lipofectamine 3000 was from Invitrogen Co.. Opti-MEM was from GIBCO Co. .

Isolation and purification of HSPCs

Mice were sacrificed by cervical dislocation. The femur was elevated and bone marrow was rinsed. The filtrate was subjected to centrifugation and pellet was suspended in red blood cell lysis buffer, followed by centrifugation at 3000 rpm, 5 min. The precipitate was bone marrow(BM) mononuclear cells (MNCs) (Fig.S1A). MNCs were next suspended in PBS containing EDTA and 0.5% BSA. Then we isolated HSPC using $Lin^{-}c\text{-}kit^{+}$ immunomagnetic beads sorting technique with lineage cell depletion kits and anti-c-Kit microbeads (Fig.S1B). All animal experiments were performed in compliance with guidelines of the Animal Care and Use Committee of SHUTCM.

The establishment and identification of HSPCs model

1) Young group: HSPCs were isolated from 4-weeks-old mouse according to the steps above;

2) aging Model group: Young HSPCs were cultured in the modeling medium (Stemspan Stem Cell Media + IL3 + IL6 + SCF) for 7 days ; and the modeling medium was changed every 2 to 3 days (Fig.S1C).

SA-β-gal staining

HSPCs (~1000,000 cells) were fixed with 4% paraformaldehyde for 15 minutes. The cells were incubated at 37ºC without CO_2 for 16 h in β-galactosidase staining solution. The number of β-galactosidase positive cells per 400 total cells was counted.

Mixed colony-forming unit (CFU-Mix) of HSPC culture

Cells (~100,000cells) were collected and subjected to CFU culture: Cells in duplicates were diluted with IMDM + 2% FBS and MethoCult™ GF M3434 medium to a final concentration of 5×103 cells per 35mm dish. 0.3 mL of the diluted cells were added to 3mL of MethoCult™ and mixed thoroughly. The final cell mixture was dispensed into each 35 mm dish at a volume of 1.1 mL and incubated at 37ºC in 5% CO2 for 7 days. Next, cells were imaged with an inverted microscope to obtain microscopical record of CFU-Mix. Then we added 1mg/ml of p-iodonitrotetrazolium violet to cells in 24-well and photographed the cells after 24 hours to acquire macroscopical images of CFU-Mix. The number of CFU-Mix per 5×103 cells represented the pluripotency of HSPCs.Realtime PCR

Total RNA extraction and reverse transcription were performed according to the manufacturer's instructions (9108/9109,Takara; RR047A, Takara). Specific primers were designed and synthesized by Sango biotech and β-actin primers were used as internal control. SYBR green kit (RR420A, Takara) was used for RT-qPCR and 2-ΔCt method was used to quantify mRNA transcripts. The amplification parameters were: 95ºC for 30 s, (95ºC for 5 s, 60ºC for 34 s) for 40 cycles. The analysis was performed with three biological replicates.

Western Blotting

Cells were lysed with RIPA lysis containing protease inhibitor and cell lysates were subjected to total protein quantification with the Bradford method (Bio-Rad). An aliquot of 70 μg of protein extract was loaded in each lane and separated in a 10% SDS-PAGE gel and electroblotted on a PVDF membrane. Membrane was then blocked with 4% BSA in 1×TBS and 0.1% TWEEN®20, washed and probed with primary antibodies for overnight at room temperature, with GAPDH as loading control. Blots were then washed and incubated with 1:2000 dilution of HRP secondary antibody for 2 h at room temperature. After wash, the protein bands were developed with the chemiluminescent reagents (Millipore). Relative band intensities were determined by using ImageJ software.

Small interfering RNA (siRNA)

Three siRNAs specifically targeting Rbmxl1 versus HnRNPa2/b1 were designed and synthesized, respectively. Cells were collected and resuspended in HSPCs medium without cytokines for transfection. 20 pM of specific siRNAs were added to 50μl of Opti-MEM serum-free medium; an equivalent amount of non-specific siRNA was added as a negative control. 1.5μl of lipofectamine 3000 (Invitrogen) reagent was added to another aliquot of 50μl Opti-MEM. Mixed the above solution for 20min and then add by dropping in 400μL of cell suspension ($0.5\text{-}2\times10^5$ per well in a 24-well plate). Upon 6 hours of transfection, cells were incubated with cytokine-free media and harvested upon 72 hours post transfection for the following assays: RT-qPCR validation of Rbmxl1 and HnRNPa2/b1 transcripts expression; and SA-β-gal staining and CFU-Mix formation assays for aging manifestation.

Cut-tag

Recombinant pA-Tn5 and pA-Tn5 transposome assembly were reported (Wang et al. 2021b). Cleavage under targets and tagmentation was performed as described previously (Kaya-Okur et al. 2019; Wang et al. 2019) with some modifications. Briefly, cells were incubated with activated concanavalin A-coated magnetic beads (Smart-Lifesciences). The bead-bound cells were permeabilized and incubated first with H3K27me3 primary antibody, followed by anti-Flag M2 antibody (Sigma-Aldrich), and lastly with rabbit anti-mouse IgG antibody. Diluted pA-Tn5 adapter complex was next added and then followed by the tagmentation reaction. DNA fragments were extracted for library preparation. More details of this experiment and data analysis are described in Supplemental Methods.

RNA-seq, Library Generation, and Bioinformatics Analysis

Briefly, mRNA was purified from total RNA using poly-T oligo-attached magnetic beads. Fragmentation was carried out using divalent cations under elevated temperature in First Strand Synthesis Reaction Buffer (5X). First strand cDNA was synthesized using random hexamer primer and M-MuLV Reverse Transcriptase (RNase H-). Second strand cDNA synthesis was subsequently performed using DNA Polymerase I and RNase H. Remaining overhangs were converted into blunt ends via exonuclease/polymerase activities. After adenylation of 3’ ends of DNA fragments, adaptors with hairpin loop structure were subjected to ligation for hybridization. In order to select cDNA fragments centered in the range of 370 ~ 420 bp in length, the library fragments were purified with AMPure XP system (Beckman Coulter, Beverly, USA). Then PCR was performed with Phusion High-Fidelity DNA polymerase,

Universal PCR primers and Index (X) Primer. At last, PCR products were purified (AMPure XP system) and library quality was assessed on the Agilent Bioanalyzer 2100 system. For GO enrichment analysis, selected differentially regulated genes between young group and old group HSPCs were analyzed on the Gene Ontology Consortium website (geneontology.org), with Fisher-test-corrected $P < 0.05$. Like GO enrichment, association of the genes with different path-ways was computed with the Kyoto Encyclopedia of Genes and Genomes (KEGG) (http://www.genome.jp/kegg) databases. Alternative splicing analysis was performed using ASprofile software. All data are representative of three independent experiments.

Patient Sample

Bone marrow (BM) samples (n = 16) were collected from healthy donors and MDS patients treated for 1-year (from April 2021 to April 2022) in the Hematology Department of the Fujian Medical University Union Hospital of China. Written informed consent was obtained from all donors and all MDS diagnoses were confirmed by dedicated hematopathologists(Fig.S2, Tab.S1). BM MNCs were isolated from each sample using the standard gradient separation approach with Ficoll-Paque PLUS (GE Healthcare Lifesciences). For cell sorting, MNCs were enriched using Lin-c-kit + immunomagnetic beads sorting technique with lineage cell depletion kits and anti-c-Kit microbeads (Fig.S1B). The study was approved by the clinical research ethics committee of Fujian Medical University Union Hospital.

Statistical analysis

The experimental data was expressed as a mean and standard deviation. The sample sizes (n) in the figure legends indicate the number of replicates in each experiment and are provided in the corresponding figure legends. Single factor analysis of variance and one-way ANOVA was performed using SPSS 18.0. The LSD or Tamhane test was used to compare differences between two groups. $p < 0.05$ was considered statistically significant.

Results

1. Association of mRNA splicing with HSPC aging

To specify the link of mRNA splicing to HSPC aging, we firstly monitored the messages of splicing factors, such as SR family members (Srsf1, Srsf2, Srsf3, Srsf4, Srsf5, Srsf6, Srsf7, Srsf9, and Srsf11) and hnRNPs family members (hnRNPI, HnRNPa0, and HnRNPa2/b1). We also assessed two additional splicing-related genes (Rbmxl1 and Pabpc1) that changed significantly in the aging model but were unknown in functionalities.

As shown, the message expression of the following genes in the aging model group were significantly lower than the control young group: Srsf1, Srsf2, Srsf3, Srsf4, Srsf6, Srsf7, hnRNPI (PTB), HnRNPa0, Pabpc1, and Rbmxl1 (Fig. 1A, $p < 0.01$). There were no significant differences in the transcripts of Srsf5, Srsf11 and HnRNPa2/b1 genes (Fig. 1A, $P > 0.05$). In accordance with mRNA expression, protein levels of the following genes in aging model HSPCs were significantly lower than the control young group: Srsf1,

Srsf2, Srsf3, Srsf5, Srsf7, Srsf11, HnRNPa2/b1, HnRNPa0, PTB, Pabpc1, and Rbmxl1 (Fig. 1B-1C, $p < 0.01$). There were no significant difference in protein expression of Srsf4 and Srsf6 genes (Fig. 1B-1C, $P > 0.05$). Together, aforementioned SR and HnRNPs genes were systemically down-regulated in the aging group, with the exception of only a few genes.

2. Rbmxl1 and HnRNP a2/b1 KD led to HSPCs aging

Next we pursued the functions of Rbmxl1 and Pabpc1 on HSPC senescence, considering both were significantly down-regulated in the aging model. For this purpose, we studied effects of Rbmxl1 or HnRNP a2/b1 siRNA knock down (KD) on aging-related manifestations. Tests in 293T cells transfected with silencing and control vectors showed high KD efficiencies (Fig. 2A). Next, SA-β-gal (Senescence-related β-galactosidase) assay and colony-forming unit (CFU)-mix assay were applied for aging-related HSPC manifestations.

SA-β-gal as a hallmark of aging can yield a blue stain in the cytoplasm of aging cells[19]. Our results showed that the percentage of SA-β-gal stain-positive cells in Rbmxl1-siRNA group was significantly higher than the control group (day 0) (Fig. 2C $P < 0.01$, $P < 0.05$). Blue-stained cells (senescent cells) were also larger than non-senescent cells, and most of the blue-stained cells showed morphological abnormalities. However, there was no significant change between HnRNPa2/b1-siRNA group and the control group (Fig. 2D, $P > 0.05$). CFU-Mix assay were next used to gain insight into the frequency and types of progenitor cells present in the - population and their ability to proliferate and differentiate. As observed in Fig. 2E-2F, no colonies was found in Rbmxl1-siRNA group and the colony numbers was decreased significantly in HnRNPa2/b1-siRNA group compared with the control group that had robust colonies, suggesting both gene are critical for HSPCs proliferation and differentiation

3. Effect of mRNA splicing inhibitor SSA on aging-related manifestations of HSPCs

Spliceostatin A (SSA), an mRNA splicing inhibitor, was next used to study whether mRNA splicing contribute to HSPC aging. In the control young group, HSPCs were isolated from 4-weeks-old mouse; in the aging Model group, cells handling was described in the Methods section; and in the SSA group, the young HSPCs were treated with 100 ng/mL SSA for 72h. SA-β-gal staining and CFU-Mix assay were performed for comparison. The results showed that the percentage of SA-β-gal stain-positive cells in SSA group was significantly higher than the control group, mimicking observations in the aging model group (Fig. 3A-3C, $P < 0.01$, $P < 0.05$). In CFU-Mix assay, no colonies was found in SSA group or in aging model group, in contrast to robust colonies in the control group (Fig. 3D-3F).

Recent reports pointed out that aging forced the differentiation of HSCs to myeloid bias. Normally, myeloid progenitor cells (MPC) differentiate into megakaryocytes (platelets), erythrocytes, granulocytes, and monocytes (macrophages); and lymphoid progenitor cells (LPC) differentiate into B cell, T cell and NK cell. In our study the CFU-Mix assay revealed the following colony types: burst-forming unit-erythroid (BFU-E), Granulocyte/ macrophage progenitor cells (CFU-GM), Colony-forming unit-granulocyte (CFU-G)

and colony-forming unit-macrophage (CFU-M), multi-potential progenitor cells (colony-forming unit-granulocyte, erythroid, macrophage, megakaryocyte, CFU-GEMM), and B lymphocyte progenitor cells (CFU-pre-B) (Fig. 3G-J). The microscopical imaging showed that the CFU-GM population increased and the CFU- GEMM population decreased in SSA group, as compared with the control group (Fig. 3K-L). Pre-B clones were found in the control group (Fig. 3M), while no pre-B clone was found in the SSA group or the aging model group.

4. Cut-tag analysis of H3K27me3 chromatin occupancy in HSPC

In our early work, total H3K27me3 was significantly down-regulated in the aging model group compared with the young group[12]. In current work, we conducted cut-tag assay to evaluate H3K27me3 expression at the chromatin loci of key mRNA splicing genes. In accordance with our report, overall H3K27me3 level in aging model group was significantly lower than the young group[12]. H3K27me3 peaked around the transcription start sites (TSS) (Fig. 4A, Fig. 4C, Fig.S3-S5). Enhancer of zeste homolog 2 (EZH2) is the catalytic subunit of polycomb repressive complex 2 (PRC2) that regulates downstream genes by catalyzing H3K27me3[20]. Significantly, we determined EZH2 transcripts were markedly down-regulated in aging HSPCs (Fig. 4B).

In cut-tag assay, Tn5 enzyme cut the open areas of chromatin. Interestingly, the number of DNA fragments in the aging model group increased in comparison to the control group, suggesting elevation in chromatin accessibility (Fig.S6). However, there were genome-wide increase of H3K27me3 peaks in the aging model group (Fig.S7, Table.1). Consistently, locus-specific occupancy of H3k27me3 was enhanced on the promoter of the following splicing factors: Srsf1, Srsf2, Srsf3, Srsf4, Srsf5, Srsf6, Srsf7, Srsf9, Srsf11, hnRNPI (PTB), HnRNP a0, HnRNP a2/b1, Rbmxl1 and Pabpc1 (Fig. 4D,Fig. 4G). The IGV diagrams were shown as Fig. 4G. Gene Ontology (GO) analysis showed enrichments in multiple RNA splicing relevant terms, in additional to regulation of hemopoiesis, hemopoiesis, definitive hemopoiesis and aging (Fig. 4E-4F).

5. Conjoint Analysis of Cut-tag and RNA-Seq datasets

We next integrated the analyses on cut-tag and RNA-Seq datasets that were developed in our early and current works. Venn chart showed that the number of overlapping genes among differential expression genes was 727 (Fig. 5A). The GO-term enrichment mainly covered the categories in mRNA splicing and hematopoiesis - (Fig. 5B-5D). Interactions Network graph based on GO:BP (biological process) demonstrated that mRNA splicing and hematopoiesis terms were both in intra-correlation but were not mutually correlated (Fig. 5E).

Next, we address the alternative splicing modes by comparing aging model and young HSPCs. Our analyses covered the following alternative splicing event types: TSS (alternative 5' first exon); TTS (alternative 3' last exon); SKIP (skipped exon); XSKIP (approximate SKIP); MSKIP (multi-exon skip); XMSKIP (approximate MSKIP); IR (intron retention); XIR (approximate IR); MIR (multi-IR); XMIR

(approximate MIR); AE (alternative exon ends); and XAE (approximate AE). The results showed that in comparison with young HSPCs, aging HSPCs exhibited significant alterations in TSS and SKIP (Table.2 and Fig. 5F-5G, $P < 0.001$).

6. Characterization of HSPC aging in MDS clinical samples

The clinical parameters of the MDS patients were shown in Tab.S2. and Fig.S3 and HSPC senescence was evaluated with CFU-Mix and SA-β-Gal assays, respectively. As shown in Fig. 6A-6B, the proportion of SA-β-gal stain-positive cells in the MDS group was significantly higher than that in the control group ($P < 0.01$, $P < 0.05$). CFU-Mix assays showed that colony numbers decreased significantly in MDS group compared with the control group (Fig. 6C). Together, both tests exposed that HSPCs in the MDS group were degraded markedly in their proliferation and differentiation capacities.

7. Gene expression profiling based on in vitro and in vivo datasets.

As we expected, transcriptomics profiling of MDS patients demonstrated that Aging was one significant differential terms in GO analysis and the Cellular Senescence pathway was one significant differential pathway in KEGG analysis (Fig. 7C-7F). The Top25 differently expressed genes in Aging Term and Cellular Senescence pathway were shown in Tab.S2 and Tab.S3; and the Cellular Senescence pathway was shown as Fig.S8. Next, we combined the *in vitro* (Aging Model HSPCs vs Young HSPCs) and *in vivo* (MDS vs normal) RNA-Seq datasets (Fig. 7G). The joint analysis showed 1444 genes, 412 GO Terms, and 22 KEGG Pathways were in overlap. Particularly, aging-relevant P21 gene was markedly up-regulated in both Aging Model and MDS groups ($P < 0.05$) (Table.3, Tab.S1-S2). In accordance, P21-related P53 signaling pathway was one overlapping KEGG Pathway ($P < 0.05$).

Discussion

In the process of mRNA splicing, a spliceosome forms first and consists of the core member (small nuclear ribonucleoprotein, snRNP) complex and auxiliary members, which mainly include hnRNPs (heterogenous ribonuclear proteins, hnRNPs) family and SR (serine/arginine, SR) proteins family[21]. SR and hnRNPs are groups of RNA-binding proteins that recognize and bind the auxiliary sites on the pre-mRNA, namely intronic or exonic splicing silencer or enhancer sequences, to promote or repress exon splicing. Under specific conditions, constitutive splicing that dominates mRNA splicing can be perturbed by alternative splicing (AS) events. During RNA maturation, AS contributes to diversity in transcripts and protein isoforms along over 95% of human genome[22–24]. Key AS regulators contain SR proteins, hnRNPs and epigenetic factors including histone modification that play distinct splicing functions[25–27]. SR family is encoded by nine genes (designated Srsf1、Srsf2、Srsf3、Srsf4、Srsf5、Srsf6、Srsf7、Srsf9、Srsf11[28]), all of which were evaluated in this study. hnRNPs have different molecular weights ranging from 34 to 120 kDa and are named alphabetically from hnRNP A1 to hnRNP U. Many hnRNPs are found

in same complexes, suggesting shared structure and/or function[29]. Here we focused on HnRNPa2/b1, HnRNPa0, and hnRNP I that had significant expression differences in our model group compared to the control young group. HnRNPa2/b1 is a key hnRNP family member[29], HnRNPa0 is in association with human peripheral blood aging phenotypes[31], and hnRNP I is implicated in histone-mark-dependent splicing[32].

Based on our findings, aforementioned SR and hnRNPs proteins systemically decreased in the aging model group in comparison with the young group. We speculated that aging-induced dysregulation of SR and hnRNPs families in HSPC reflected loss of alternative splicing diversity upon HSPC senescence[33]. We also determined two additional mRNA splicing-related genes (Rbmxl1 and Pabpc1) were both markedly down-regulated in the aging model group. The followed siRNA KD tests indicated that Rbmxl1-KD led to CFU-Mix inhibition and SA-β-gal activation, all indicating extreme aging[34]. Although our tests demonstrated that Rbmxl1-KD would induce HSPC senescence, HnRNP a2/b1-KD resulted in decrease in colony-forming but no change in SA-β-gal activity. Interestingly, HSPCs of the SSA group showed a similar phenotype to HSPCs in the aging model group, i.e., the increase in SA-β-Gal positive cell population without colony formation. These findings reflected decline in the proliferation and differentiation capacities of HSPCs in the SSA group. Under normal conditions, HSCs would differentiate into balanced myeloid and lymphoid lineages, but aging could force the differentiation of HSCs to myeloid bias[36]. Consistently, microscopical observation by CFU-mix assay affirmed HSPCs of the SSA group differentiated into myeloid with some extent of disproportion.

Dysregulation of splicing factor(SF) expression was emerging as a driver of aging[35, 38], and in primary human fibroblasts, replicative and oxidative stress-induced senescence models bore dysregulation of 58 genes associated with RNA splicing at the pre-senescence stage[37]. Functional links exist between histone modifications and alternative splicing and can be bidirectional[39, 41]. H3K27me3 is an important epigenetics marker catalyzed by the PRC2 to inhibit transcriptional elongation and silence target genes[40]. The cut-tag results showed that promoter-specific enrichment of H3K27me3 on chromatin and overall decrease of H3K27me3 in the aging HSPC in comparison to the young HSPC, in accordance with our early report[12]. However, global down-regulation of H3K27me3 appeared to be incompatible to its enhanced occupancy at the following gene loci: Srsf1, Srsf2, Srsf3, Srsf4, Srsf5, Srsf6, Srsf7, Srsf9, Srsf11, hnRNPI, HnRNPa0, HnRNPa2/ b1, Rbmxl1 and Pabpc1. We also analyzed changes in alternative splicing modes in aging HSPCs and found changes in SR and HnRNPs levels leaded to AS of downstream targets, driving one of the following patterns: TSS and SKIP. It was reported that H3K27me3 functions in the alternative splicing mode [42–43], and based our findings of H3K27me3 enrichment at the promoter sites indicated its potential functions in alternative splicing of 5' first exon in the TSS mode. Collectively, we reconcile these findings by proposing site-specific epigenetics regulation at chromatin level.

The clinical data showed a strong correlation of MDS morbidity rates with by age, with the mid-age of 77[17, 30, 44]. Here we highlighted the activities of HSPC aging in MDS etiopathology by assessing clinical

HSPCs. Significantly, the HSPCs of MDS patients showed marked increase in SA-gal positive rate and decrease in CFU-Mix colony number. Transcriptomics confirmed aging as one significant differential Terms in GO analysis and cellular senescence as one key impacted pathway in KEGG analysis. In addition, both our *in vivo* and *in vitro* studies consistently pointed that expression of aging-related p21/CDKN1A was substantially increased. Indeed, up-regulation of p21 was showed in coupling to the primary response-inducing cellular senescence[45–47]. Another perturbed effector is the P53 pathway, which could inhibit senescence by antagonizing the expression p21[48].

Conclusion

In summary, with our patent *in vitro* HSPCs aging mouse model, we assessed HSPC senescence mechanisms with focuses on mRNA splicing and epigenetics. We determined that HSPCs aging was associated with repression of mRNA splicing-related genes through enhanced promoter occupancy of H3k27me3. Consequently, alternative splicing modes including TSS and SKIP were evoked for alternative splicing of 5' first exon. This study also substantialized the relevance of HSPC senescence to MDS pathogenesis, highlighting the role of HSPC aging in MDS etiopathology.

Abbreviations

MDS Myelodysplastic Syndromes

HSCs hematopoietic stem cells

HSPC Hematopoietic stem/progenitor cell

KD knock down

CFU Colony-Forming Unit

BM bone marrow

MNCs mononuclear cells

SSA Spliceostatin A

MPC myeloid progenitor cells

LPC lymphoid progenitor cells

BFU-E burst-forming unit-erythroid

GM Granulocyte/ macrophage progenitor cells

CFU-G Colony-forming unit-granulocyte

CFU-M Colony-forming unit-macrophage

GEMM granulocyte, erythroid, macrophage, megakaryocyte

pre-B B lymphocyte progenitor cells

TSS transcription start sites

EZH2 Enhancer of zeste homolog 2

PRC2 polycomb repressive complex 2

GO Gene Ontology

BP biological process

Declarations

Acknowledgements

We thank Shaoyong Chen for critically reading and revise the manuscript.

Funding

This work was supported by the National Natural Science Foundation of China (No. 82074274), the Fujian Province Natural Science Foundation (No.2019J01159), National Key Clinical Specialty Discipline Construction Program(No.2021-76) and Fujian Provincial Clinical Research Center for Hematological Malignancies（No.2020Y2006). The roles of the funding body involved in the design of the study and collection, analysis, and interpretation of data and in writing the manuscript.

Availability of data and materials

All data generated or analyzed during this study are included in this published article.

Authors' Contributions

H.Y.H. developed the approaches, performed the experiments, analyzed the data. X.R.S. helped to analyze the data and revised the manuscript. L.Z. helped to perform the experiments. L.Y.H. and Y.J.L. assisted with clinical sample, data collection, and performed the in vitro experiments. C.X. and M.Y.Z. collected and analyzed the data. X.L.L. and L.N.Z. developed the concepts and approaches, supervised the entire study including experimental design and data analysis, prepared and revised the manuscript. All authors read and approved the final manuscript.

Competing interests

The authors declare no conflicts of interest.

Ethics approval and consent to participate

This study was approved by the clinical research ethics committee of Fujian Medical University Union Hospital, Fuzhou, China. All animal works were carried out in compliance with the ethical regulations and guidelines approved by the Animal Care Committee of SHUTCM.

Consent for publication

All the patients that involved in the study have given their consent to publish their individual data.

Publisher's Note

Springer Nature remains neutral with regard to jurisdictional claims in published maps and institutional affiliations.

Open Access

References

1. Gazit R, Weissman IL, Rossi DJ. Hematopoietic stem cells and the aging hematopoietic system. Semin Hematol. 2008;45(4):218-224. doi:10.1053/j. seminhe- matol.2008.07.010
2. Osorio FG, Rosendahl Huber A, Oka R, Mark Verheul, Sachin H Patel, Karlijn Hasaart,et al. Somatic Mutations Reveal Lineage Relationships and Age-Related Mutagenesis in Human Hematopoiesis. Cell Rep. 2018;25(9): 2308-2316.e4. doi:10.1016/j.celrep.2018.11.014
3. Konieczny J, Arranz L. Updates on Old and Weary Haematopoiesis. Int J Mol Sci. 2018;19(9):2567. Published 2018 Aug 29. doi:10.3390/ijms19092567
4. Yu KR, Espinoza DA, Wu C, Lauren Truitt , Tae-Hoon Shin, Shirley Chen,et al. The impact of aging on primate hematopoiesis as interrogated by clonal tracking. Blood. 2018;131(11):1195-1205. doi:10.1182/blood-2017-08-802033

5. Snoeck HW. Aging of the hematopoietic system. Curr Opin Hematol. 2013;20(4):355-361. doi:10.1097/MOH.0b013e3283623c77
6. Shlush LI. Age-related clonal hematopoiesis. Blood. 2018;131(5):496-504. doi:10.1182/blood-2017-07-746453
7. Lee J, Yoon SR, Choi I, Jung H. Causes and Mechanisms of Hematopoietic Stem Cell Aging. Int J Mol Sci. 2019;20(6):1272. Published 2019 Mar 13. doi:10.3390/ijms20061272
8. Zhang SS, Dong F, Cheng T, Hideo E. Zhongguo Shi Yan Xue Ye Xue Za Zhi. 2018;26(3):637-641. doi:10.7534/j.issn.1009-2137.2018.03.001
9. Luis TC, Tremblay CS, Manz MG, North TE, King KY, Challen GA. Inflammatory signals in HSPC development and homeostasis: Too much of a good thing?. Exp Hematol. 2016;44(10):908-912. doi:10.1016/j.exphem.2016.06.254
10. Abkowitz JL, Catlin SN, McCallie MT, Guttorp P. Evidence that the number of hematopoietic stem cells per animal is conserved in mammals. Blood. 2002;100(7):2665-2667. doi:10.1182/blood-2002-03-0822
11. Dykstra B, de Haan G. Hematopoietic stem cell aging and self-renewal. Cell Tissue Res. 2008;331(1):91-101. doi:10.1007/s00441-007-0529-9
12. Dong Y, Guo C, Zhou W, Li W, Zhang L. Using a new HSPC senescence model in vitro to explore the mechanism of cellular memory in aging HSPCs. Stem Cell Res Ther. 2021;12(1):444. Published 2021 Aug 9. doi:10.1186/s13287-021 -02455-x
13. Deschênes M, Chabot B. The emerging role of alternative splicing in senescence and aging. Aging Cell. 2017;16(5):918-933. doi:10.1111/acel.12646
14. Bhadra M, Howell P, Dutta S, Heintz C, Mair WB. Alternative splicing in aging and longevity. Hum Genet. 2020;139(3):357-369. doi:10.1007/s00439-019- 02094-6
15. Wang K, Wu D, Zhang H, et al. Comprehensive map of age-associated splicing changes across human tissues and their contributions to age-associated diseases. Sci Rep. 2018;8(1):10929. Published 2018 Jul 19. doi:10.1038/s41598-018- 29086-2
16. de Almeida SF, Grosso AR, Koch F, Romain Fenouil, Sílvia Carvalho, Jorge Andrade,et al. Splicing enhances recruitment of methyltransferase HYPB/Setd2 and methylation of histone H3 Lys36. Nat Struct Mol Biol. 2011;18(9):977-983. Published 2011 Jul 26. doi:10.1038/nsmb.2123
17. Chung SS, Park CY. Aging, hematopoiesis, and the myelodysplastic syndromes. Blood Adv. 2017;1(26):2572-2578. Published 2017 Dec 8. doi:10.1182/b loodadvances.2017009852
18. Montalban-Bravo G, Garcia-Manero G. Myelodysplastic syndromes: 2018 update on diagnosis,risk-stratification and management. Am J Hematol. 2018;93(1):129-147. doi:10.1002/ajh. 24930
19. Bassaneze V, Miyakawa AA, Krieger JE. Chemiluminescent detection of senescence-associated β galactosidase. Methods Mol Biol. 2013;965:157-163. doi:10.1007/978-1-62703-239-1_9
20. Duan R, Du W, Guo W. EZH2: a novel target for cancer treatment. J Hematol Oncol. 2020;13(1):104. Published 2020 Jul 28. doi:10.1186/s13045- 020- 00937-8.

21. Kędzierska H, Piekiełko-Witkowska A. Splicing factors of SR and hnRNP families as regulators of apoptosis in cancer. Cancer Lett. 2017;396:53-65. doi:10.1016/j.canlet.2017.03.013
22. Gueroussov S, Gonatopoulos-Pournatzis T, Irimia M, Bushra Raj, Zhen-Yuan Lin, Anne-Claude Gingras,et al. An alternative splicing event amplifies evolutionary differences between vertebrates. Science. 2015;349(6250):868 -873. doi:10.1126/science.aaa8381
23. Wu J, Lu G, Wang X. MDM4 alternative splicing and implication in MDM4 targeted cancer therapies. Am J Cancer Res. 2021;11(12):5864-5880. Published 2021 Dec 15.
24. Pan Q, Shai O, Lee LJ, Frey BJ, Blencowe BJ. Deep surveying of alternative splicing complexity in the human transcriptome by high-throughput sequencing [published correction appears in Nat Genet. 2009 Jun;41(6):762]. Nat Genet. 2008;40(12):1413-1415. doi:10.1038/ng.259
25. Busch A, Hertel KJ. Evolution of SR protein and hnRNP splicing regulatory factors. Wiley Interdiscip Rev RNA. 2012;3(1):1-12. doi:10.1002/wrna.100
26. Erkelenz S, Mueller WF, Evans MS, Anke Busch, Katrin Schöneweis, Klemens J Hertel, et al. Position-dependent splicing activation and repression by SR and hnRNP proteins rely on common mechanisms [published correction appears in RNA. 2013 Jul;19(7):1015]. RNA. 2013;19(1):96-102. doi:10.1261/rna.037044.112
27. Kędzierska H, Piekiełko-Witkowska A. Splicing factors of SR and hnRNP families as regulators of apoptosis in cancer. Cancer Lett. 2017;396:53-65. doi:10.1016/j.canlet.2017.03.013
28. Shepard PJ, Hertel KJ. The SR protein family. Genome Biol. 2009;10(10):242. doi:10.1186/gb-2009-10-10-242
29. Geuens T, Bouhy D, Timmerman V. The hnRNP family: insights into their role in health and disease. Hum Genet. 2016;135(8):851-867. doi:10.1007/s00439- 016-1683-5
30. Hu D, Yuan S, Zhong J, et al. Cellular senescence and hematological malignancies: From pathogenesis to therapeutics. Pharmacol Ther. 2021;223:107817. doi:10.1016/j.pharmthera. 2021.107817
31. Lee BP, Pilling LC, Bandinelli S, Ferrucci L, Melzer D, Harries LW. The transcript expression levels of HNRNPM, HNRNPA0 and AKAP17A splicing factors may be predictively associated with ageing phenotypes in human peripheral blood. Biogerontology. 2019;20(5):649-663. doi:10.1007/s10522-019-09819-0
32. Xue Y, Zhou Y, Wu T, Tuo Zhu, Xiong Ji, Young-Soo Kwon, Chao Zhang, et al. Genome-wide analysis of PTB-RNA interactions reveals a strategy used by the general splicing repressor to modulate exon inclusion or skipping. Mol Cell. 2009;36(6):996-1006. doi:10.1016/j.molcel. 2009.12.003
33. Harries LW, Hernandez D, Henley W, Andrew R Wood, Alice C Holly, Rachel M Bradley-Smith, et al. Human aging is characterized by focused changes in gene expression and deregulation of alternative splicing. Aging Cell. 2011;10(5):868-878. doi:10.1111/j.1474-9726.2011. 00726.x
34. Nygaard HB, Erson-Omay EZ, Wu X, Brianne A Kent , Cecily Q Bernales , Daniel M Evans ,et al. Whole-Exome Sequencing of an Exceptional Longevity Cohort. J Gerontol A Biol Sci Med Sci. 2019;74(9):1386-1390. doi:10.1093/gerona/ gly098

35. Lee BP, Pilling LC, Emond F, Kevin Flurkey, David E Harrison, Rong Yuan , et al. Changes in the expression of splicing factor transcripts and variations in alternative splicing are associated with lifespan in mice and humans. Aging Cell. 2016;15(5):903-913. doi:10.1111/acel.12499
36. Lee J, Yoon SR, Choi I, Jung H. Causes and Mechanisms of Hematopoietic Stem Cell Aging. Int J Mol Sci. 2019;20(6):1272. Published 2019 Mar 13. doi:10.3390/ijms20061272
37. Bhadra M, Howell P, Dutta S, Heintz C, Mair WB. Alternative splicing in aging and longevity. Hum Genet. 2020;139(3):357-369. doi:10.1007/s00439- 019-02094-6
38. Kwon SM, Min S, Jeoun UW, Min Seok Sim, Gu Hyun Jung, Sun Mi Hong,et al. Global spliceosome activity regulates entry into cellular senescen- ce. FASEB J. 2021;35(1):e21204. doi:10.1096/fj.202000395RR
39. Luco RF, Pan Q, Tominaga K, Blencowe BJ, Pereira-Smith OM, Misteli T. Regulation of alternative splicing by histone modifications. Science. 2010;327 (5968):996-1000. doi:10.1126/science.1184208
40. Schuettengruber B, Bourbon HM, Di Croce L, Cavalli G. Genome Regulation by Polycomb and Trithorax: 70 Years and Counting. Cell. 2017;171(1):34-57. doi:10.1016/j.cell.2017.08.002
41. Kim S, Kim H, Fong N, Erickson B, Bentley DL. Pre-mRNA splicing is a determinant of histone H3K36 methylation. Proc Natl Acad Sci U S A. 2011;108(33):13564-13569. doi:10.1073/pnas.1109475108
42. Alló M, Buggiano V, Fededa JP, Ezequiel Petrillo, Ignacio Schor, Manuel de la Mata, et al. Control of alternative splicing through siRNA-mediated transcriptional gene silencing. Nat Struct Mol Biol. 2009;16(7):717-724. doi:10.1038/nsmb.1620
43. Sims RJ 3rd, Millhouse S, Chen CF, Brian A Lewis, Hediye Erdjument-Bromage, Paul Tempst, et al. Recognition of trimethylated histone H3 lysine 4 facilitates the recruitment of transcription postinitiation factors and pre-mRNA splicing. Mol Cell. 2007;28(4):665-676. doi:10.1016/j.molcel.2007.11.010
44. Ogawa S. Genetics of MDS. Blood. 2019;133(10):1049-1059. doi:10.1182/blood-2018 -10-844621
45. Ju Z, Choudhury AR, Rudolph KL. A dual role of p21 in stem cell aging. Ann N Y Acad Sci. 2007;1100:333-344. doi:10.1196/annals.1395.036
46. Zhang Y, Shao C, Li H,Kun Wu, Lixin Gong , Quan Zheng, et al. The Distinct Function of p21Waf1/Cip1 With p16Ink4a in Modulating Aging Phenotypes of Werner Syndrome by Affecting Tissue Homeostasis. Front Genet. 2021;12:597566. Published 2021 Feb 5. doi:10.3389/fgene.2021.597566
47. López-Domínguez JA, Rodríguez-López S, Ahumada-Castro U, Pierre-Yves Desprez, Maria Konovalenko, Remi-Martin Laberge, et al. Cdkn1a transcript variant 2 is a marker of aging and cellular senescence. Aging (Albany NY). 2021;13(10):13380-13392. doi:10.18632/aging.203110
48. von Muhlinen N, Horikawa I, Alam F, Kazunobu Isogaya, Delphine Lissa, Borek Vojtesek, et al. p53 isoforms regulate premature aging in human cells. Oncogene. 2018;37(18):2379-2393. doi:10.1038/s41388-017-0101-3

Tables

Tables 1 to 3 are available in the Supplementary Files section

Figures

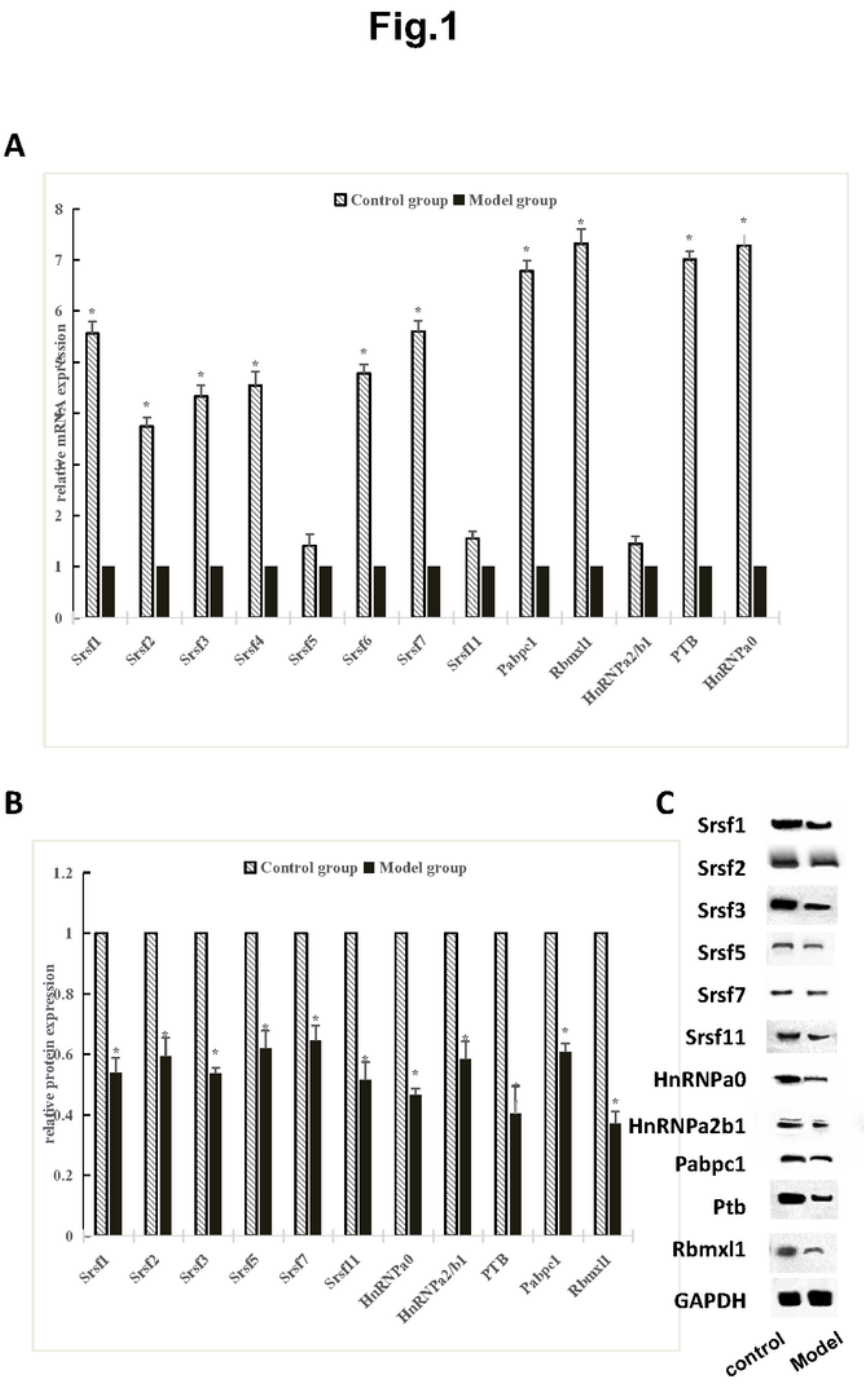

Figure 1

Altered message and protein expressions of SR and hnRNPs family genes in aging HSPCs. (A) Realtime-qPCR was used to measure the transcripts of SR and hnRNPs genes. (B,C) Western blotting was used to measure the proteins of SR and hnRNPs genes.

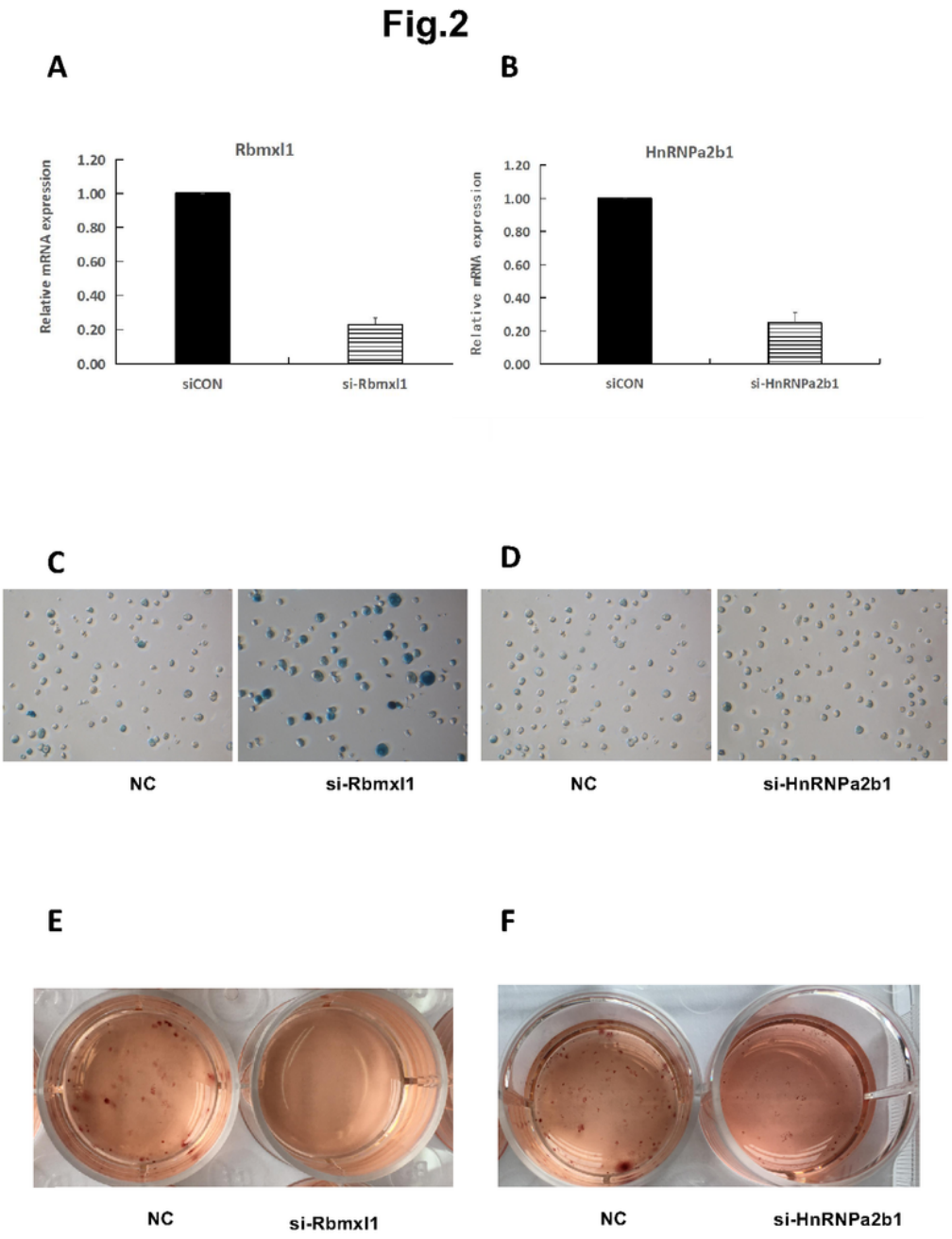

Figure 2

Effects of Rbmxl1 and HnRNP a2/b1 KD in HSPC on aging-related manifestations in β-galactosidase activity and colony forming capacity. HSPCs isolated from 4-weeks-old mice were treated with Rbmxl1 and HnRNPa2/b1specific siRNAs. Rbmxl1 gene expression (A) and HnRNPa2/b1 gene expression (B) were validated by RT-qPCR analysis. In comparison to the young group, SA-β-gal stained cells increased in Rbmxl1-siRNA group (C), but not in the HnRNPa2/b1-siRNA group (D); Colony-forming capacity of HSPCs significantly decreased in both Rbmxl1-siRNA group (E) and HnRNPa2/b1-siRNA group (F).

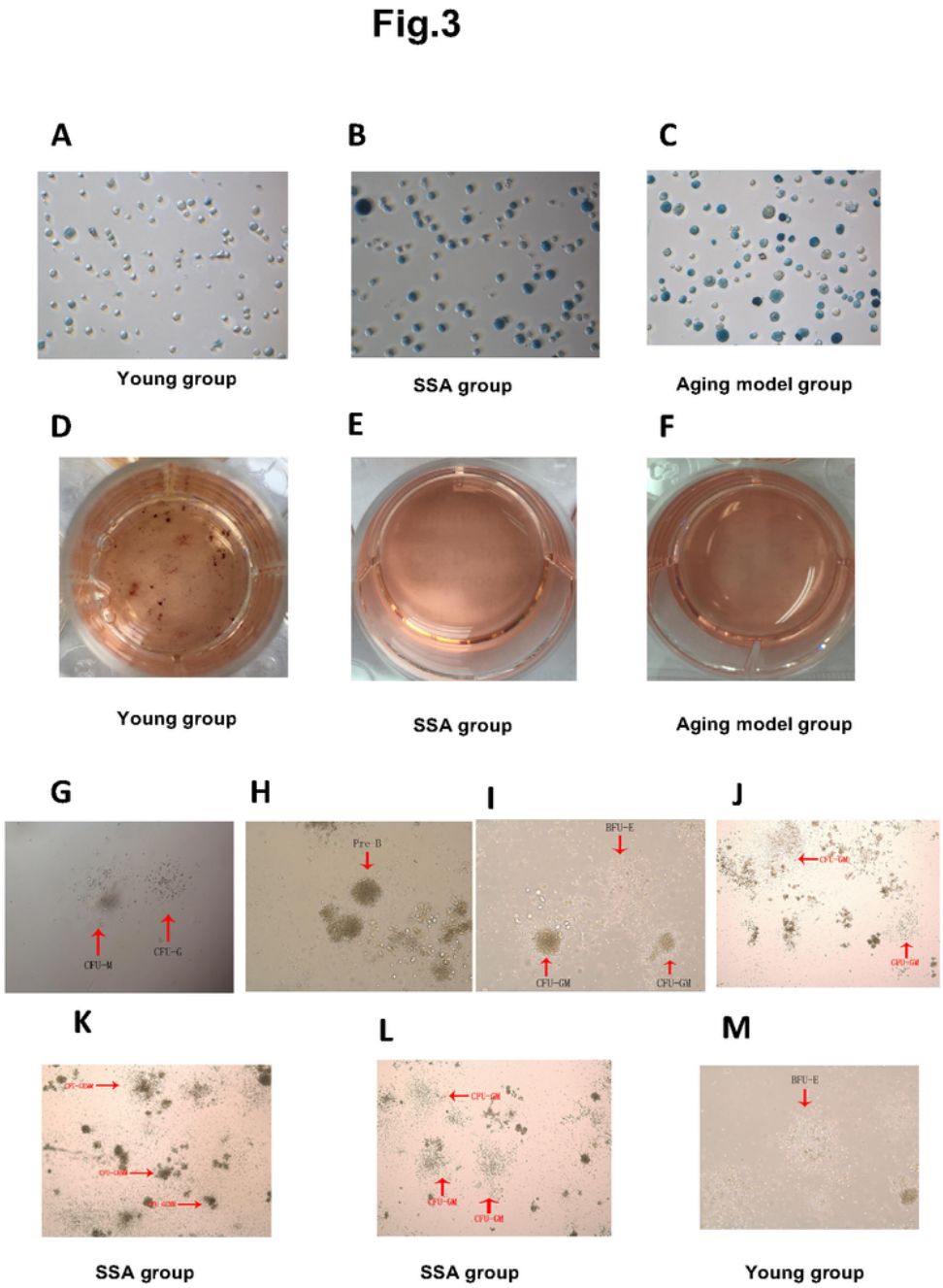

Figure 3

Effect of mRNA splicing inhibitor, SSA, on aging-related manifestations in HSPC. In comparison with the control group (A), SA-β-gal stained cells increased in SSA group (B) and Aging model group (C). As compared with the control group (D), colony-forming ability of HSPCs significantly decreased in both SSA group (E) and aging model group (F). List of microscopical photographs: CFU-Mix (G, H, I, J, K, L, M); CFU-G and CFU-M (G, 100x); Pre-B (H, 200x, Young control group); BFU-E (I, 200x), CFU-GM (J, 40x, SSA group), CFU-GEMM (K, 40x, Young control group), CFU-GM (L, 40x, Aging model group), and BFU-E (M,200x).

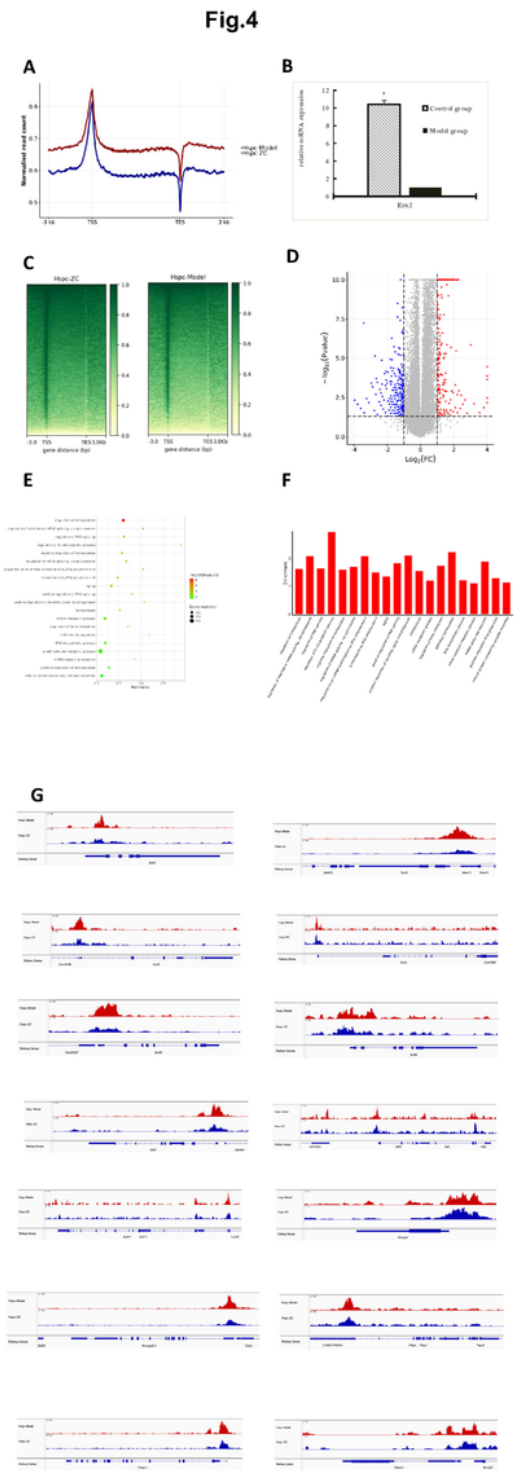

Figure 4

Cut-tag analysis of H3K27me3 genomic occupancy in HSPC. (A) Distribution of reads on genome-wide scale. We normalized all genes according to their lengths and calculated the average H3K27me3 signals between TSS (−3 kb) and TES (+ 3 kb) of all genes. TSS, transcription start site; TES, transcription end site. (B) RT-PCR analysis of EZH2 transcripts. (C) Heatmap plotting of H3K27me3 binding signals across ± 3 kb from all genes in HSPCs and color intensity reflects binding affinity. (D) Volcano plotting to

visualize result for differential binding peaks. Blue dots represents down-regulated peaks and red dots represents up-regulated peaks. (E) GO bubble chart for relevant up-regulated peak genes: X-axis represents Rich factor and Y-axis represents GO term. The size of dot represents number of genes and the color of dot represents p-value. (F) GO enrichment bar for relevant up-regulated peak genes. X-axis represents GO term and Y-axis represents enrichment. (G) Snapshot of specific gene IGV diagrams, indicating systemic enhancement in H3K27me3 affinity in aging model group as compared with the young group.

Fig.5

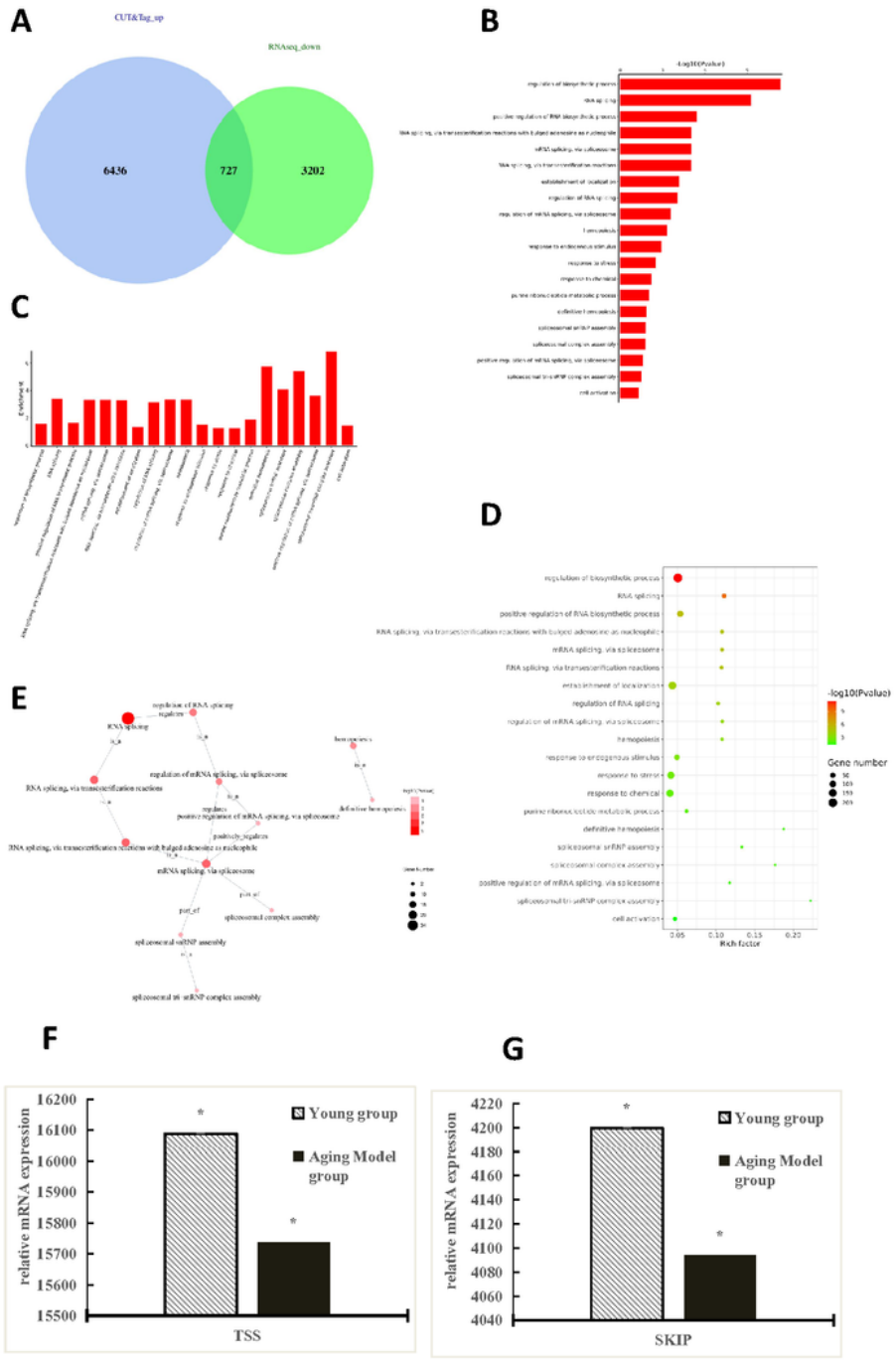

Figure 5

Conjoint Analysis of Cut-tag and RNA-Seq datasets. (A) Wayne chart; (B) GO p-Value analysis of overlapping genes; (C) GO enrichment analysis of overlapping genes; (D) GO bubble chart of overlapping genes; (E) GO BP graph of interaction networks.

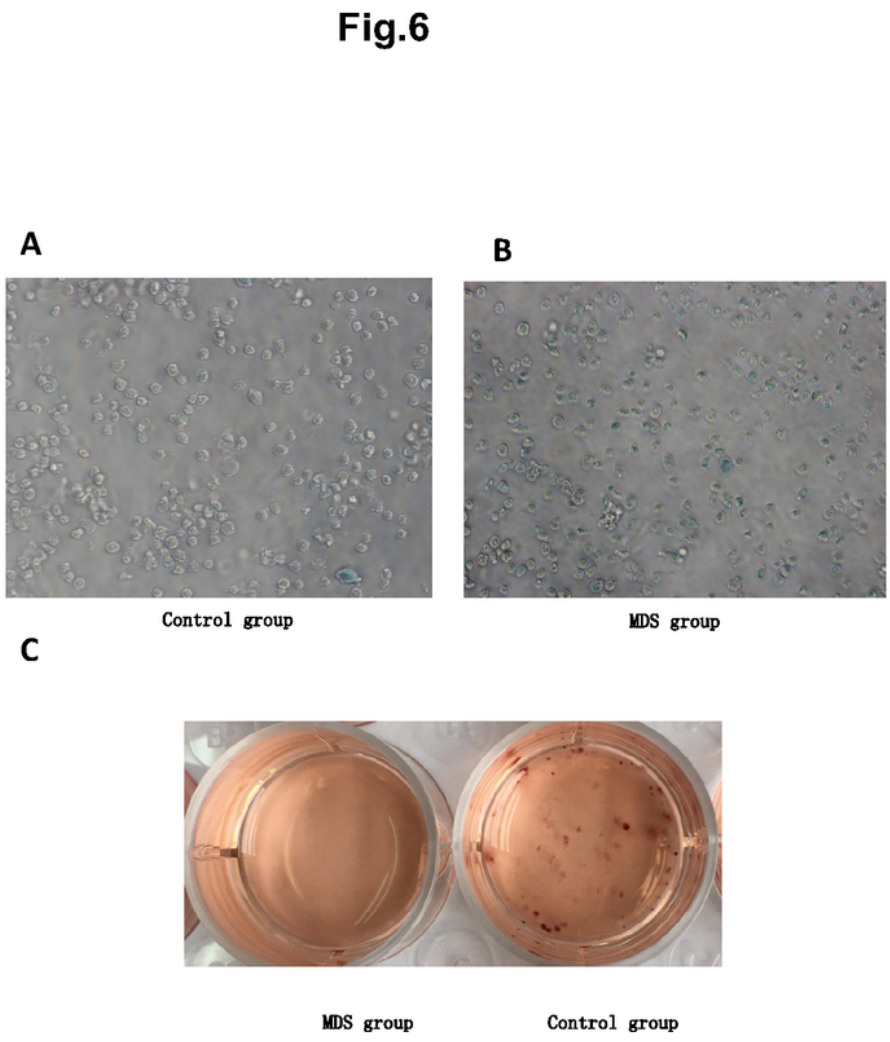

Figure 6

HSPC aging related evaluation in MDS clinical samples. (A-B) compared with control group, SA-β-gal stain-positive cells increased in the MDS group. (C) Colony-forming ability of HSPCs in the MDS group significantly decreased in comparison with the control group.

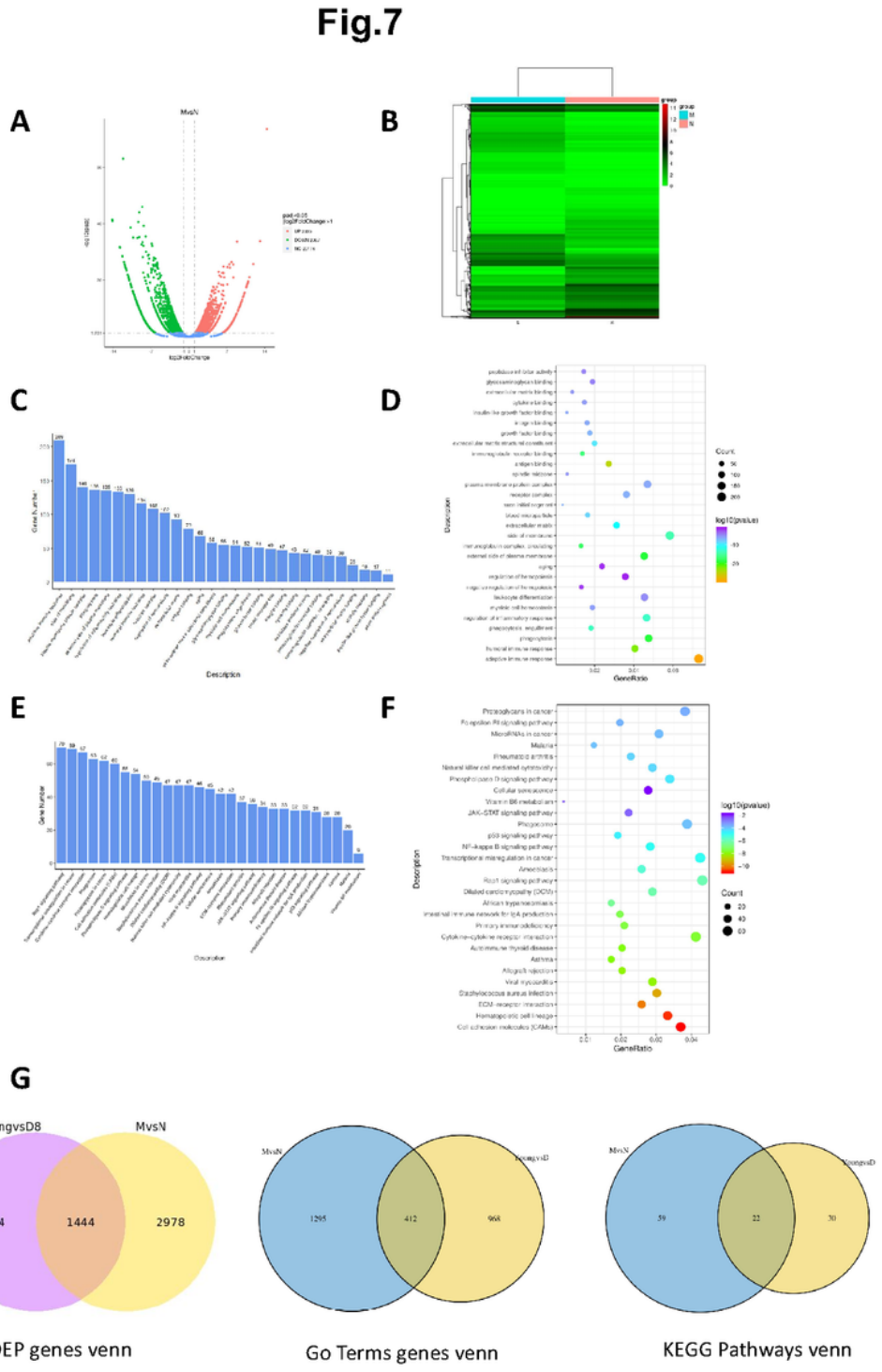

Figure 7

RNA-Seq analysis of MDS clinical samples. (A) Volcano plotting of transcriptomes. Red color represented the up-regulated genes and green color represents down-regulated genes, respectively. (B) Cluster analysis. (C) GO enrichment bar. (D) GO bubble chart. (E) KEGG enrichment bar. (F) KEGG bubble chart. As shown, aging and cellular senescence pathways were among top-ranked differential pathways in enrichment analysis; in addition, negative regulation of hemopoiesis and regulation of hemopoiesis and hematopoietic cell lineage were also highly enriched. **Conjoint analyses of *in vitro* and *in vivo* RNA-Seq datasets(Fig.7G).**

Supplementary Files

This is a list of supplementary files associated with this preprint. Click to download.

- 20220829Supplementaryfile.pptx
- 20220829Table.pptx